



Hydrologic Alteration and Enhanced Microbial Reductive Dissolution of Fe(III) (hydr)oxides Under Flow Conditions in Fe(III)-Rich Rocks: Contribution to Cave-Forming Processes

Kayla A. Calapa¹, Melissa K. Mulford², Tyler D. Rieman³, John M. Senko^{1,2,3}, Augusto S. Auler⁴, Ceth W. Parker⁵ and Hazel A. Barton^{1,2,3*}

¹ Department of Biology, University of Akron, Akron, OH, United States, ² Integrated Bioscience, University of Akron, Akron, OH, United States, ³ Department of Geosciences, University of Akron, Akron, OH, United States, ⁴ Instituto do Carste, Belo Horizonte, Brazil, ⁵ Planetary Protection Center of Excellence, NASA Jet Propulsion Laboratory, Pasadena, CA, United States

OPEN ACCESS

Edited by:

Sujun Li,
Indiana University, United States

Reviewed by:

James F. Holden,
University of Massachusetts Amherst,
United States
Xiaolong Liang,
Washington University in St. Louis,
United States

*Correspondence:

Hazel A. Barton
bartonh@uakron.edu

Specialty section:

This article was submitted to
Microbiological Chemistry
and Geomicrobiology,
a section of the journal
Frontiers in Microbiology

Received: 16 April 2021

Accepted: 21 June 2021

Published: 14 July 2021

Citation:

Calapa KA, Mulford MK,
Rieman TD, Senko JM, Auler AS,
Parker CW and Barton HA (2021)
Hydrologic Alteration and Enhanced
Microbial Reductive Dissolution
of Fe(III) (hydr)oxides Under Flow
Conditions in Fe(III)-Rich Rocks:
Contribution to Cave-Forming
Processes.
Front. Microbiol. 12:696534.
doi: 10.3389/fmicb.2021.696534

Previous work demonstrated that microbial Fe(III)-reduction contributes to void formation, and potentially cave formation within Fe(III)-rich rocks, such as banded iron formation (BIF), iron ore and canga (a surficial duricrust), based on field observations and static batch cultures. Microbiological Fe(III) reduction is often limited when biogenic Fe(II) passivates further Fe(III) reduction, although subsurface groundwater flow and the export of biogenic Fe(II) could alleviate this passivation process, and thus accelerate cave formation. Given that static batch cultures are unlikely to reflect the dynamics of groundwater flow conditions *in situ*, we carried out comparative batch and column experiments to extend our understanding of the mass transport of iron and other solutes under flow conditions, and its effect on community structure dynamics and Fe(III)-reduction. A solution with chemistry approximating cave-associated porewater was amended with 5.0 mM lactate as a carbon source and added to columns packed with canga and inoculated with an assemblage of microorganisms associated with the interior of cave walls. Under anaerobic conditions, microbial Fe(III) reduction was enhanced in flow-through column incubations, compared to static batch incubations. During incubation, the microbial community profile in both batch culture and columns shifted from a Proteobacterial dominance to the Firmicutes, including Clostridiaceae, Peptococcaceae, and Veillonellaceae, the latter of which has not previously been shown to reduce Fe(III). The bacterial Fe(III) reduction altered the advective properties of canga-packed columns and enhanced permeability. Our results demonstrate that removing inhibitory Fe(II) via mimicking hydrologic flow of groundwater increases reduction rates and overall Fe-oxide dissolution, which in turn alters the hydrology of the Fe(III)-rich rocks. Our results also suggest that reductive weathering of Fe(III)-rich rocks such as canga, BIF, and iron ores may be more substantial than previously understood.

Keywords: cave (speleogenic) and alluvial deposits (formations), iron reduction bacteria, hydrology and water, *Desulfosporosinus*, *Veillonella*

INTRODUCTION

The Southern Espinhaço Mountain Range (SE) of southeastern Brazil contains commercially important, high-grade iron ore hosted by the Serra da Serpentina Group, a stratigraphic unit which includes the iron-rich Serra do Sapó Formation (Auler et al., 2019). These sedimentary units were formed by the precipitation of Fe(III) and Si phases from solution during the Proterozoic Eon (Weber et al., 2006; Rosière et al., 2019; Silveira Braga et al., 2021). Iron ores can include magnetite (Fe_3O_4), hematite ($\alpha\text{-Fe}_2\text{O}_3$), or a ferric oxyhydroxide like goethite ($\alpha\text{-FeOOH}$) or limonite ($\text{FeO}(\text{OH})\cdot n(\text{H}_2\text{O})$), and high-grade ore averages between 60 and 67% Fe (Dorr, 1964; Beukes et al., 2003; Rolim et al., 2016). The SE and Quadrilátero Ferrífero (Iron Quadrangle; QF) located ~150 km south of SE, contain abundant Fe(III)-rich minerals, which can be found in intact banded iron formation (BIF), Si-depleted ore, and canga rock (Beukes et al., 2003; Souza et al., 2015; Auler et al., 2019). BIF contains alternating bands of quartz (SiO_2) and either magnetite or hematite that range from a few millimeters to a few centimeters in thickness, and averages between 15 and 38% iron (Smith, 2015; Rolim et al., 2016). Canga is a brecciated duricrust containing clasts of iron oxide (usually BIF) with an iron-oxide cement matrix that averages between 57 and 62% iron (Dorr, 1964; Spier et al., 2007; Gagen et al., 2019). Canga contains the most poorly crystalline Fe(III) of the three major phases (i.e. canga, BIF, and ore), with goethite the most prominent mineral phase (Parker et al., 2013).

Canga and BIF are generally considered highly resistant to both mechanical and chemical weathering at $\text{pH} \geq 3$ (Dorr, 1964; Johnson et al., 2012; Auler et al., 2014; Spier et al., 2018; Gagen et al., 2019), and canga covers the slopes and valleys of the SE region. Yet this area is also associated with hundreds of caves (iron formation caves; IFCs) that form mostly at the BIF/canga boundary (Auler et al., 2019). The identification of these caves suggests that processes leading to Fe(III) weathering and removal increase porosity at the canga/BIF interface, despite the resistance of both types of rocks to dissolution. At circumneutral pH, Fe solubility can be enhanced by microbially mediated reductive dissolution of Fe(III) phases to relatively soluble Fe(II). This activity may facilitate the mass transport necessary for the increased porosity and the formation of the observed IFCs (Parker et al., 2013, 2018). In support of this hypothesis, while the walls of the IFCs are lined with a hard, oxidized layer of canga, the interior (approximately 3 cm behind) of the wall surface contains a soft, goeey, water-saturated material that contains abundant microbial cells (Parker et al., 2018). Given the inhibition of Fe-reduction by oxygen, we wondered whether this material was involved in promoting Fe-reduction and increased porosity, leading to formation of the IFCs. Canga is a rather porous media, and active vertical percolation of water occurs during rainfall, the patterns of which can be irregular, depending on season (Mesquita et al., 2017; Parker et al., 2018). As such, intermittent periods of extensive water circulation around and within caves and their hosting rocks can occur, followed by water stagnation or dry periods.

Prior enrichment of canga-associated microorganisms from IFCs demonstrated that the microbial communities present were capable of Fe(III) reduction to extents that could contribute to IFC formation (Parker et al., 2018), but Fe(II) that accumulates during Fe(III) (hydr)oxide reduction can adsorb to Fe(III) phase surfaces and induce mineral (trans)formations (Roden et al., 2000; Benner et al., 2002; Hansel et al., 2003, 2005; Gonzalez-Gil et al., 2005). These consequences of Fe(III) reduction could self-limit further Fe(III) (hydr)oxide reduction, although subsurface water flow could help overcome these limitations by advective transport of Fe(II) (Gonzalez-Gil et al., 2005; Minyard and Burgos, 2007; Wefer-Roehl and Kübeck, 2014). Additionally, it remained unclear if the extents of microbiological Fe(III) (hydr)oxide dissolution observed were sufficient to induce hydrologic alterations that would culminate in cave formation. To understand whether this hydrologic flow could influence Fe-reduction rates and enhance IFC formation we compared batch cultures [where Fe(II) will accumulate] to columns [where Fe(II) is removed via flow] to evaluate how water flow influenced microbiologically mediated Fe(III) reduction, and whether such activity could influence the hydraulic properties of canga.

MATERIALS AND METHODS

Sample Collection and Preparation for Batch Incubations and Column Experiments

Five IFCs were sampled in the SE region of Brazil in December 2018. The cave designations are: CSS-0009, CSS-0080, CSS-0010, CSS-0107, and CSS-0074. Authorization for sampling during the destruction of these caves through mining had been approved by the Brazilian environmental agency, and the sampling was part of a final recovery effort prior to mining. Canga was collected from the interior of a cave that was forming at a BIF-canga interface. Large (0.5–5.5 kg) chunks of canga were removed from cave walls using an electric demolition hammer during the final sampling effort prior to cave destruction and placed in plastic bags. The soft, microbial-rich material behind the walls (*sub muros*) was collected by first removing the rigid oxide layer and then using a sterile garden shovel to place this material in sterile glass jars and sealed with plastic tape to maintain anaerobic/microaerobic conditions. Samples were placed in a refrigerator upon return from the field. Collected canga was pulverized for column experiments by cutting large chunks into smaller pieces with a water-cooled trim saw with a 25 cm blade, which were then processed through a ball mill (SPEX Industries, Inc., Metuchen, NJ, United States) until all the material passed through a 1.44 mm sieve. This pulverized canga was sterilized by autoclaving at 121°C for 15 min, allowing a 1 h recovery, and then autoclaved again to assure deactivation of spore-forming bacteria. This sterilized canga was then dried at 65°C for 14–16 h in an oven.

Batch Incubations

Preparation of batch incubations was carried out in a Coy anaerobic glove bag (Coy Laboratory Products, Inc., Grass Lake, MI, United States) filled with 3–5% H₂, balance N₂. Synthetic porewater (SPW) composition was based on characterization of IFC porewaters, and contained 5 mM CaCl₂, 0.1 mM Na₂SO₄, and 0.1 mM KH₂PO₄. Sodium lactate (5.0 mM) was included as an electron donor and carbon source, and the pH of the SPW was adjusted to either pH 4.75 or pH 6.8 with HCl or NaOH, respectively, which were chosen to approximate the pH of porewaters we have observed in IFCs (Parker et al., 2018). O₂ was removed from the SPW by bringing the liquid to nearly boiling, then cooling under a stream of N₂ gas for 45 min. Once cooled, SPW-containing bottles were sealed, transferred to the anaerobic glove bag, and filter-sterilized with a 0.2 μm PES filter (VWR, Radnor, PA, United States) until use in incubation bottles or column experiments. Batch sediment incubations contained 20 g of pulverized canga (equivalent to approximately 120 mmol Fe(III)) and 60 mL of SPW in 160 mL serum bottles that were sealed with butyl rubber stoppers held in place with aluminum crimp seals. Where appropriate, 5 g of *sub muros* material and associated microbial community was used as inoculum for non-sterile incubations. Incubations were carried out in triplicate.

Column Assembly and Operation

All materials used for packing columns were acid-washed and sterilized prior to use, and all columns (10 cm × 1 cm Econo-Columns; Bio-Rad Laboratories, Hercules, CA, United States) were packed and operated in a Coy anaerobic glove bag as described. Approximately 2 g of 3 and 2 mm diameter glass beads were placed at the bottom of the column, respectively, to prevent sediment clogging. The uninoculated columns were packed with pulverized sterile canga using a “lift” technique: a 2 g lift of canga was added, followed by the injection of 200–500 μL SPW (described above) through bottom of the column. After the addition of each lift, the columns were tapped to remove air bubbles, and sediments were allowed to settle for 1–2 min. A suspension of *sub muros* was prepared with 8 g pulverized canga and 8 g *sub muros* in 6 mL SPW, which was added 250 μL at a time after each lift of canga/SPW during column packing. The final amount of *sub muros* added was ~2 mL, which resulted in ~9.2 × 10⁷ cells/g column material (as determined by direct cell counting; see below). All columns received 4 g of 2 mm beads followed by 2 g of 3 mm beads added to on top of the sediments to prevent clogging. After packing, columns contained a total of 16 g of solids and 7 mL liquid (either SPW only in uninoculated columns or SPW and microbial suspension in inoculated columns). All column incubations were carried out in triplicate in the anaerobic glove bag for 14 days prior to the first sampling.

Synthetic porewater was delivered to columns in an upward flow during sampling using a Masterflex L/S Precision Variable-Speed Console peristaltic pump with Masterflex L/S 8-Channel Pump Head (Cole-Parmer, Vernon Hills, IL, United States), and 1.6 mm inner diameter Tygon tubing (Fischer Scientific, Pittsburgh, PA, United States). The columns were subsequently

incubated statically for 7 days at room temperature between sampling events, whereupon 3–5 column void volumes of SPW were passed through at a flow rate of 0.2 mL/min, and during this period samples were collected from each column volume for measurement of pH, sulfate concentration, and dissolved Fe(II) concentration (described below). At the completion of the experiments, breakthrough curves were determined with 1 mM NaBr-amended (Acros Organics, Morris, NJ, United States) SPW at a flow rate of 0.2 mL/min, and samples were periodically collected for bromide quantification (described below). At the conclusion of the experiments, columns were deconstructed and sediments were removed for analysis of the microbial communities and quantification of total Fe(II) and microbial cells.

Sample Processing and Analytical Techniques

Column effluent samples for dissolved Fe(II) quantification were preserved in 0.5 M HCl, while those intended for measurement of pH, sulfate, and bromide were untreated. Solids were removed from the samples by centrifugation at 12,100 × g for 5 min. To measure solid-associated Fe(II) in column sediments, approximately 0.5 g of material was placed in microcentrifuge tubes with 1 mL 0.5 M HCl (Lovley and Phillips, 1987) and solids were then separated from the solution by centrifugation before measurement of Fe(II) in the supernatant. Fe(II) was quantified by ferrozine assay (Stookey, 1970). pH was measured using a SevenGo Pro pH/Ion meter (Mettler Toledo, Columbus, OH, United States). Sulfate, bromide, phosphate, nitrate, and chloride were measured by ion chromatography with a Dionex DX-120 System with an IonPac AS22 Column and conductivity detection (Thermo Fisher Scientific, Waltham, MA, United States). To analyze the mineralogy of the column at the end of the experiment, approximately 1 mL of column contents were dried in a closed container with CaCl₂ (Acros Organics, Morris, NJ, United States) as a drying agent under anaerobic conditions. Mineral characterization of the homogenized rock was determined by X-Ray Diffraction (XRD) with a Rigaku Ultima IV (Rigaku, Woodlands, TX, United States). Samples were analyzed with a 2θ between 5° and 70° and diffraction patterns were compared to those standards available on the American Mineralogist Crystal Structure Database (Downs and Hall-Wallace, 2003).

Microbial Community Analysis

Microbial cells in the *sub muros* inoculum, batch incubations, and in the columns at the conclusion of the experiments were enumerated by direct cell counting. Briefly, ~1 g samples were collected while the columns remained in the anaerobic glove bag and mixed with 1 mL of filter-sterilized Dulbecco pH 7.4 phosphate buffered saline (PBS) (Thermo Fisher Scientific, Waltham, MA, United States) and vigorously shaken by hand to mix the contents. One hundred microliter of this mixture was then added to 9.9 mL sterile PBS and 1X thiazole green DNA stain (Biotium, Fremont, CA, United States). This mixture was incubated in the dark for 30 min at room temperature and then

filtered onto a 0.2 μm GTBP Isopore polycarbonate membrane filter via a Millipore stainless steel filtration unit (Millipore Sigma, Darmstadt, Germany). The filter was removed and placed on a glass slide with 25 μL SlowFade Gold Antifade Mountant with DAPI (Thermo Fisher Scientific, Waltham, MA, United States) and cells were counted using a BX53 fluorescent microscope (Olympus America Inc., Center Valley, PA, United States). The total cell number was calculated based on 100 fields-of-view (FOV) at 1,000 \times magnification, with the average number of cells per FOV multiplied by the total dilution factor, area of the filter membrane, and standardized against the absolute weight of the material/g (Hershey et al., 2018).

For DNA analyses, genomic DNA was extracted from samples using either then DNeasy PowerLyzer PowerSoil or PowerBiofilm Kit (Qiagen, Germantown, MD, United States). Subsamples from the triplicate batch incubations were pooled before DNA extraction. PCR amplification of the 16S rRNA V3 and V4 regions using the primers 806R (5'-GGA CTA CHV GGG TWT CTA AT-3') and 515F (5'-GTG CCA GCM GCC GCG GTA A-3'), with samples identified using unique barcodes along with Illumina adapter sequences (Integrated DNA Technologies, Coralville, IA, United States). Amplification was using a Mastercycler Nexus Gradient (Eppendorf, Enfield, CT, United States), including a 3 min 94°C hot start, followed by 30 cycles of: denaturing at 94°C for 45 s, annealing at 50°C for 60 s, and then a 72°C extension for 90 s, followed by a final extension step at 72°C for 10 min. The PCR products were gel purified, and quantified using a Qubit dsDNA HS Assay Kit (Life Technologies, Waltham, MA, United States). Samples were then sequenced on an Illumina MiSeq and de-multiplexed in QIIME2 (version 2020.2; Bolyen et al., 2019) using *cutadapt demux*-paired and a quality check was carried out using *q2-deblur-denoise-16S* and *quality-filter-q-score*. OTU picking and taxonomic assignments were completed using the *feature-classifier-classify-sklearn* (Bolyen et al., 2019).

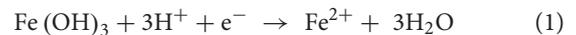
RESULTS AND DISCUSSION

Fe(III) Reduction in Static Incubations

To evaluate the canga-Fe(III) reducing activities of the microbial communities in the *sub muric* material, static batch incubations were conducted. Canga was provided as the Fe(III) source with SPW at a pH of 4.75 or 6.8, which matched the measured pH values *in situ* (Parker et al., 2018). Minimal Fe(II) was generated in uninoculated incubations, but accumulated in the *sub muros*-inoculated incubations at both pH 4.75 and 6.8 (Figure 1A). The concentration of dissolved Fe(II) that accumulated in the *sub muros*-inoculated batch incubations (approximately 5 mM) exceeded previous batch incubation work in which *Shewanella oneidensis* MR-1 was used to catalyze canga-Fe(III) reduction (less than 0.6 mM; Parker et al., 2013). Indeed, mean total Fe(II) concentration of *sub muros*-inoculated incubations exceeded 80 mmol/L (Figure 1B). In previous work, a maximum of 3% of canga-Fe(III) could be reduced by *S. oneidensis* MR-1 (Parker et al., 2013); however, greater extents of Fe(III) reduction have been observed by fermentative enrichments and isolates from canga by ourselves and other researchers (Parker et al., 2018;

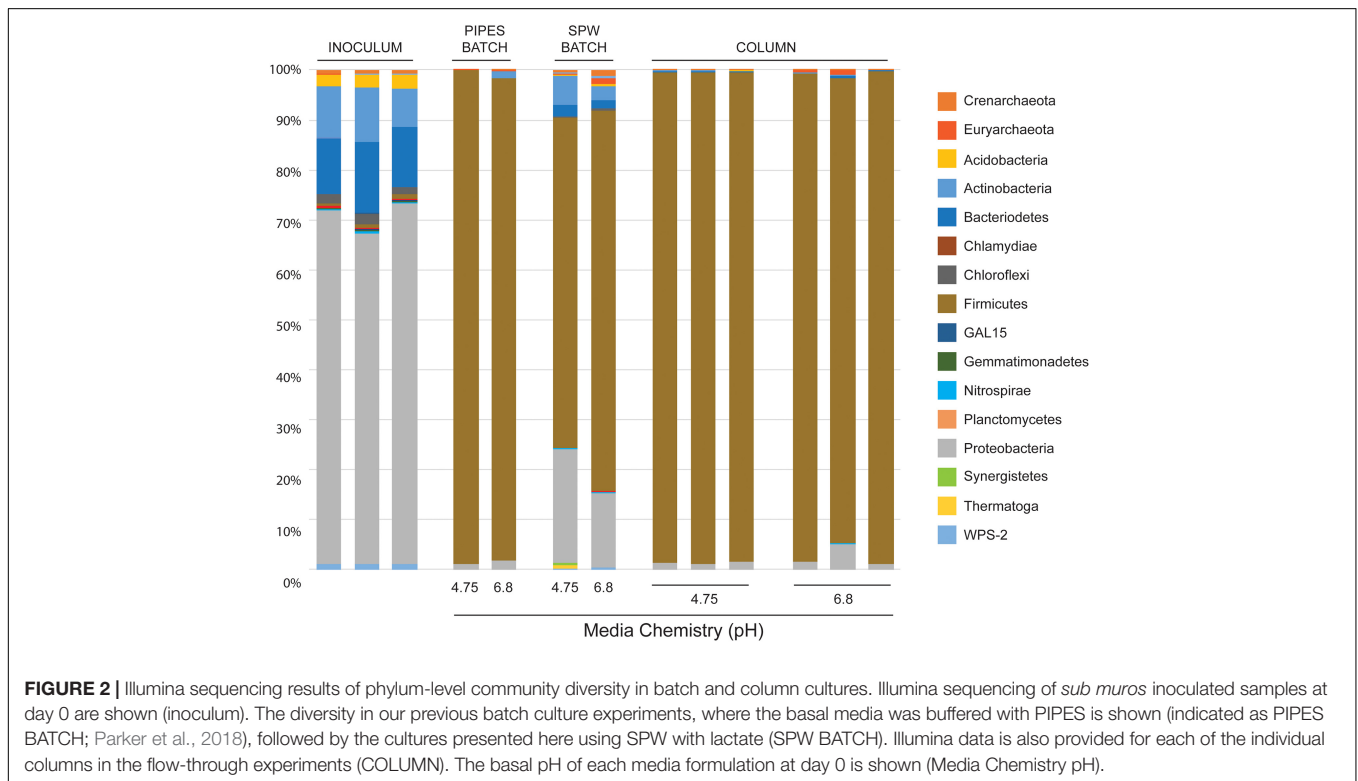
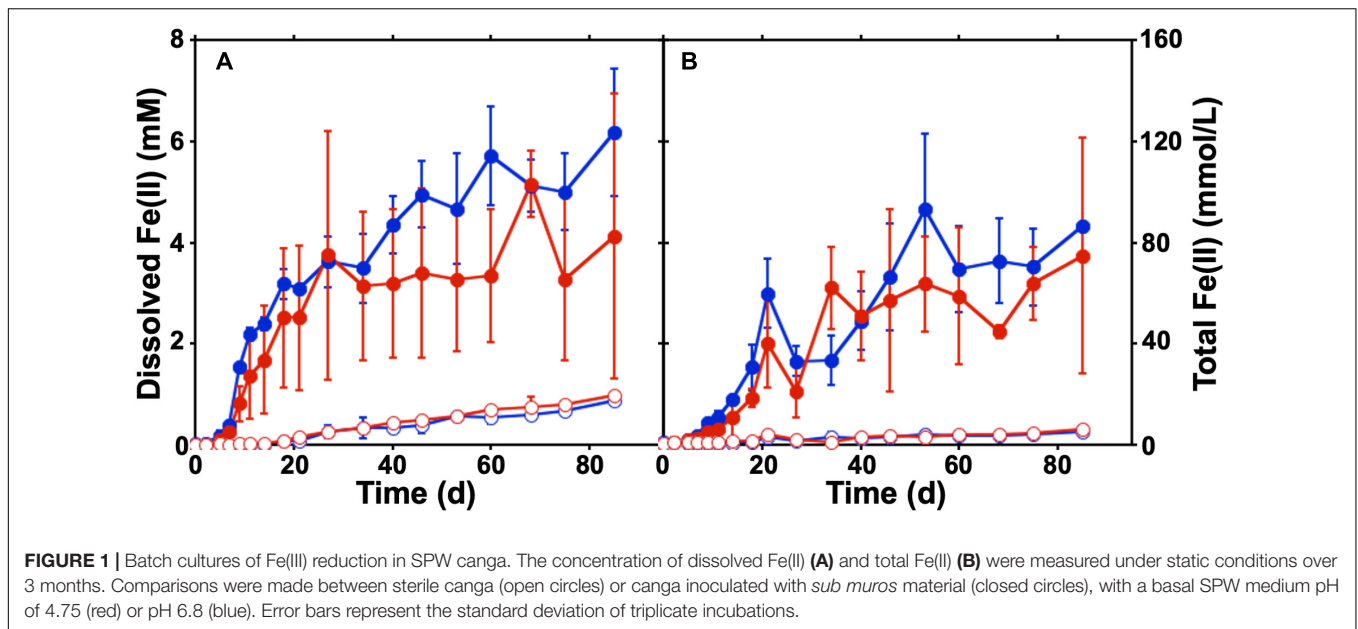
Gagen et al., 2019). The drivers of this enhanced reduction remain unclear at this time and represent a good target for future research.

In previous cultures using various Fe(III) mineral phases (including canga; Parker et al., 2018) we used a PIPES-buffered (also at pH 4.75 and 6.8) mineral salts medium for growth. In these cultures we saw a shift in microbial community structure from the Proteobacteria-dominated *sub muros* to one dominated by the Firmicutes, representing >97% of sequences (Figure 2). In these previous experiments, we had assumed that the shift in community structure had been driven in part by the high amount of organic carbon, while the closed nature of the experiment allowed H₂ to accumulate and drive fermentative Fe-reduction by members of the Clostridia (Shah et al., 2014; Parker et al., 2018). We tested this hypothesis in this study, using a basal medium (SPW) and 5 mM lactate as a carbon source. Analysis of partial 16S rRNA gene sequences in the batch incubations after 85 days revealed a similar dominance by fermentative Firmicutes (Figure 2). Nonetheless, using SPW/lactate, the Proteobacteria remained abundant, comprising 23 and 15% of the sequences recovered from pH 4.75 and 6.8 incubations, respectively. We also saw a small, but significant population of Actinobacteria (6% at pH 4.75 and 3% at pH 6.8) and Bacteroidetes (2.5% only at pH 6.8) that had not been observed previously (Figure 2). The pH of the uninoculated controls averaged 5.44, regardless of whether the pH 4.75 or 6.8 SPW was used to initiate the experiment, suggesting that canga buffered the pH; however, in the inoculated batch cultures, the SPW/lactate pH 4.75 culture increased to pH 6.10, while the SPW pH 6.8 culture remained reasonably constant at pH 6.67. There was no dramatic change in pH of the cultures following the addition of *sub muros* at day 0. This suggests Fe(III) reduction through microbial activity likely raises the pH (Eq 1):



The similarity in pH of the final culture conditions may explain the similarity of the final observed community profiles (Figure 2).

At the genus level within the dominant Firmicutes (Figure 3), the SPW/lactate batch cultures displayed a different structural diversity to our previous work. Previously, at pH 4.75 the batch cultures were dominated by members of the genus *Clostridium* (Family Clostridiales; 71%), with a small but significant representation by the *Desulfosporosinus* (Family Peptococcaceae; 6%), while at pH 6.8, the PIPES batch cultures were dominated by both the *Desulfosporosinus* (38%) and *Clostridium* (36%) (Parker et al., 2018). Both cultures also contained minor populations of the *Paenibacilli* (Family Bacillales; 3% at both pH 4.75 and 6.8). In the batch cultures presented here, we saw a similar dominance by members of the Clostridia (31% at pH 4.75 and 47% at pH 6.8), and *Desulfosporosinus* (20 and 24% at pH 4.75 and 6.8, respectively). The *Desulfosporosinus* sp. are normally associated with sulfate reduction, but have also been shown to reduce Fe(III) enzymatically (Senko et al., 2009; Sato et al., 2019). If not enzymatic, the production of a minor amount of sulfide could be sufficient to enable Fe(III) reduction via S as an electron shuttle (Hansel et al., 2015). Members of the *Paenibacilli*, which have recently been demonstrated to play an



important role in iron oxide weathering in soils (including in Brazil; Loyaux-Lawniczak et al., 2019) were also represented at both pH 4.75 and 6.8 (4% of total diversity; **Figure 3**). Interestingly, we saw a higher percentage of members of the *Coproccoccus* (Family Lachnospiraceae; 2%) at both pH 4.75 and 6.8. The genus *Coproccoccus* includes strict anaerobes that play an important role in carbohydrate fermentation in the mammalian rumen, including lactate (Rainey, 2009). It is unclear

as to why members of this genus would be enriched under the batch culture conditions; however, their growth is stimulated by fermentable carbohydrates, suggesting that the use of lactate may have enhanced their growth (Cotta and Forster, 2006; Rainey, 2009). Members of this genus have not been associated with Fe-reduction, or isolated from iron-rich environments, although the production of H₂ during fermentation may contribute to the overall culture Fe-reduction conditions (Cotta and Forster, 2006;

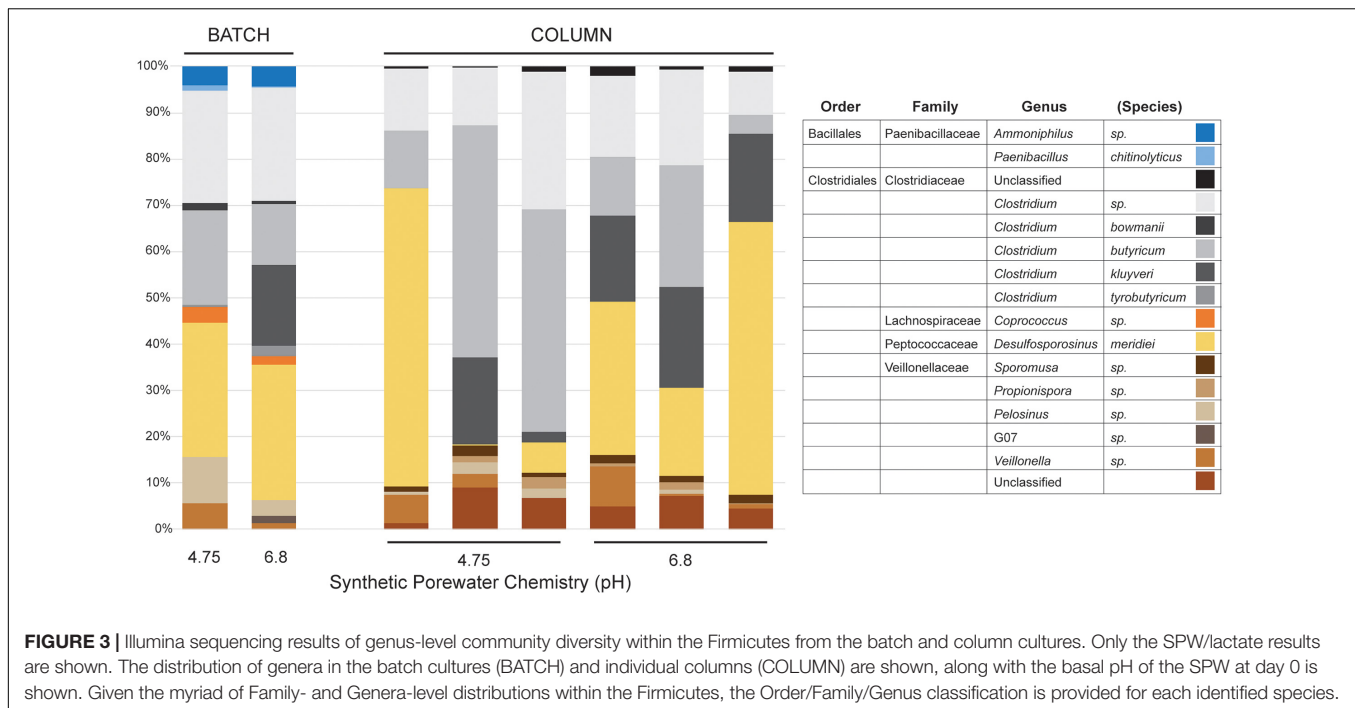


FIGURE 3 | Illumina sequencing results of genus-level community diversity within the Firmicutes from the batch and column cultures. Only the SPW/lactate results are shown. The distribution of genera in the batch cultures (BATCH) and individual columns (COLUMN) are shown, along with the basal pH of the SPW at day 0 is shown. Given the myriad of Family- and Genera-level distributions within the Firmicutes, the Order/Family/Genus classification is provided for each identified species.

Parker et al., 2018). We also observed a significant representation by members of the Family Veillonellaceae, with 11% at pH 4.75 and 5% at pH 6.8 (Figure 3). Recently, genera within the Veillonellaceae, such as *Sporomusa* spp. and *Propionispora* spp., have been shown to carry out Fe(III) reduction (Sass et al., 2004; Kato et al., 2015); however, rather using respiratory Fe(III) reduction, the *Sporomusa* appear to use Fe(III) as an electron sink in acetogenesis (Igarashi and Kato, 2021).

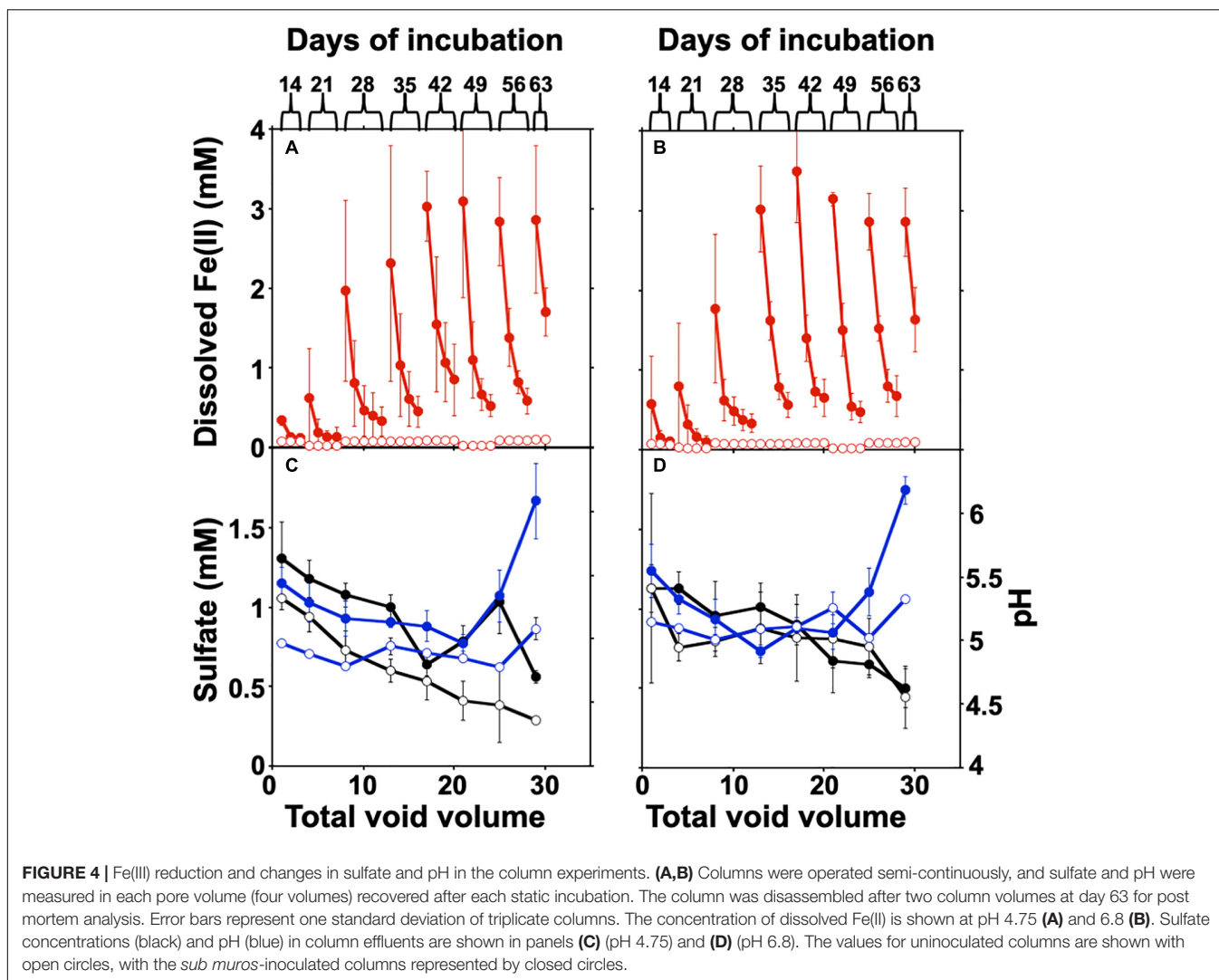
Fe(III) Reduction in Column Incubations

The underlying hypothesis of our work is that microbiological Fe(III) reducing activities are sufficient to induce porosity generation within the host rocks (i.e., canga, BIF, and iron ore); however, we have not observed hydrologic alterations of cave hosting rocks. Biogenic Fe(II) can limit the extent of Fe(III) (hydr)oxide reduction (Roden and Zachara, 1996; Urrutia et al., 1999; Roden and Urrutia, 2002; Roden, 2004, 2006), and induce mineralogical changes that would otherwise limit further Fe(III) reduction or limit the export of soluble Fe(II) (i.e., the formation of secondary minerals; Benner et al., 2002; Hansel et al., 2003, 2005). Nonetheless, the advective removal of biogenic Fe(II) as water flows through Fe(III) (hydr)oxide-rich rocks could enhance their reduction (Roden and Urrutia, 1999; Roden et al., 2000; Royer et al., 2004; Minyard and Burgos, 2007). For example, 95% of Fe(III) coating on sand was reduced over six months by *Shewanella putrefaciens* CN32 in flow-through columns, compared to 13% of the Fe(III) in batch incubations (Roden et al., 2000).

The climate regime in the SE area is highly seasonal, with over 80% of the ~1,400 mm/year rainfall concentrated in November–March. Canga is a highly porous rock, with values between 24 and 29% (Costa and Sá, 2018), while the friable ore underneath

the canga is highly impermeable with values as low as 10^{-8} m/s (Mesquita et al., 2017). Thus, rainfall infiltrates quickly through the canga towards the caves and then drains rapidly toward the surface, with very little retention of water, except in a few shallow internal ponds. Despite the robust Fe(III) reducing activity observed in the batch incubations (Figure 1; Parker et al., 2018), they do not mimic the hydrologic flow associated with the rocks of the SE or QF in which cave formation occurs with Fe(II) accumulating in the cultures. To mimic flow conditions in a laboratory setting, we packed canga into columns under conditions analogous to the batch incubations, and introduced flow into the system. This approach allowed us to answer the two major questions of this work: (1) does advective removal of biogenic Fe(II) enhance further canga-Fe(III) reduction and (2) are the Fe(III) reducing microbial activities associated with the *sub muric* material sufficient to induce hydrologic alterations to the host rock.

The columns were packed with crushed canga alone, or with crushed canga mixed with *sub muric* material. The columns were incubated statically for 14 days, allowing Fe(III) reduction to initiate, before four column volumes of SPW were then passed through the column and collected separately for analysis of effluent chemistry (Figure 4). This process of static incubation followed by introduced flow was then repeated at 7 day intervals. Minimal dissolved Fe(II) was detected in the effluent of uninoculated control columns throughout the incubation (Figure 4), and effluent pH was ~4.5–5.0, regardless of influent SPW pH. This is slightly lower than the values obtained in the batch experiments shown in Figure 1. In the inoculated columns, progressively higher concentrations of dissolved Fe(II) accumulated over the course of the incubation, with maximum Fe(II) concentrations of approximately 3 mM Fe(II) detected



after the fifth round of static incubation at both pH 4.75 and 6.8 (**Figures 4A,B**).

The concentration of total Fe(II) (dissolved and solid-associated) produced in the columns incubated at either pH 4.75 or 6.8 SPW are shown in **Table 1**. A two-sample *t*-test assuming unequal variances suggested that there was no significant difference ($P = 0.97$) in total dissolved Fe(II) accumulation in the columns receiving SPW with pH 4.75 and 6.8 (**Figure 4**). The pH of the column effluent suggests that there was an increase in pH above 6.0 (**Figure 4C**), similar to the batch cultures. The increase in Fe(III) reduction in the pH 4.75 column as the experiment progressed may reflect a change in column community structure as the cultures move toward similar pH conditions. The increase in pH conditions is correlated with the increasing observation of *Clostridium kluyveri* (**Figure 3**) and may suggest either the selection of this species under these pH conditions, or a role in driving Fe(III)-reduction.

While canga is composed mostly of goethite and poorly crystalline Fe(III) (hydr)oxides (Parker et al., 2013), if we assume dissolved Fe(II) is derived from Fe(OH)₃, approximately 40 mg

of Fe(OH)₃ were reductively dissolved and exported as Fe(II) from the packing material of inoculated columns, with minimal export of Fe from uninoculated columns (**Table 1**). In the batch

TABLE 1 | Post mortem analysis of column contents.

	pH 4.75 with <i>sub muros</i>	pH 4.75 uninoculated	pH 6.8 with <i>sub muros</i>	pH 6.8 uninoculated
Total Fe(II) ($\mu\text{mol/g}$)	60 \pm 15	4.4 \pm 0.2	89 \pm 19	4.3 \pm 0.1
Cell abundances $t = 0$ (cell/g wet)	9.3 $\times 10^7 \pm$ 2.3 $\times 10^5$	N/D	9.1 $\times 10^7 \pm$ 1.8 $\times 10^5$	N/D
Cell abundances $t = 63$ (cell/g wet)	4.0 $\times 10^8 \pm$ 8.1 $\times 10^7$	N/D	4.2 $\times 10^8 \pm$ 4.7 $\times 10^7$	N/D
Fe(OH) ₃ removed as Fe ²⁺ (mg)	38 \pm 18	2.3 \pm 0.2	40 \pm 3.5	2.3 \pm 0.01

incubations, only ~ 30 mg of $\text{Fe}(\text{OH})_3$ were reductively dissolved (Figure 1). After two porewater replacement events (21 days), the dissolved Fe(II) concentration in effluent from *sub muros*-inoculated columns exceeded 6 mM in total in pH 6.8 columns and over 5 mM total in pH 4.75 columns; iron reduction levels which only accumulated after 60 days continuous culture in batch incubations (Figures 1A, 4A,B). These results indicate that water flow enhances the reductive solubilization of Fe from canga and separation of the Fe(II) products from solid phases.

Microbial Communities in Column Incubations

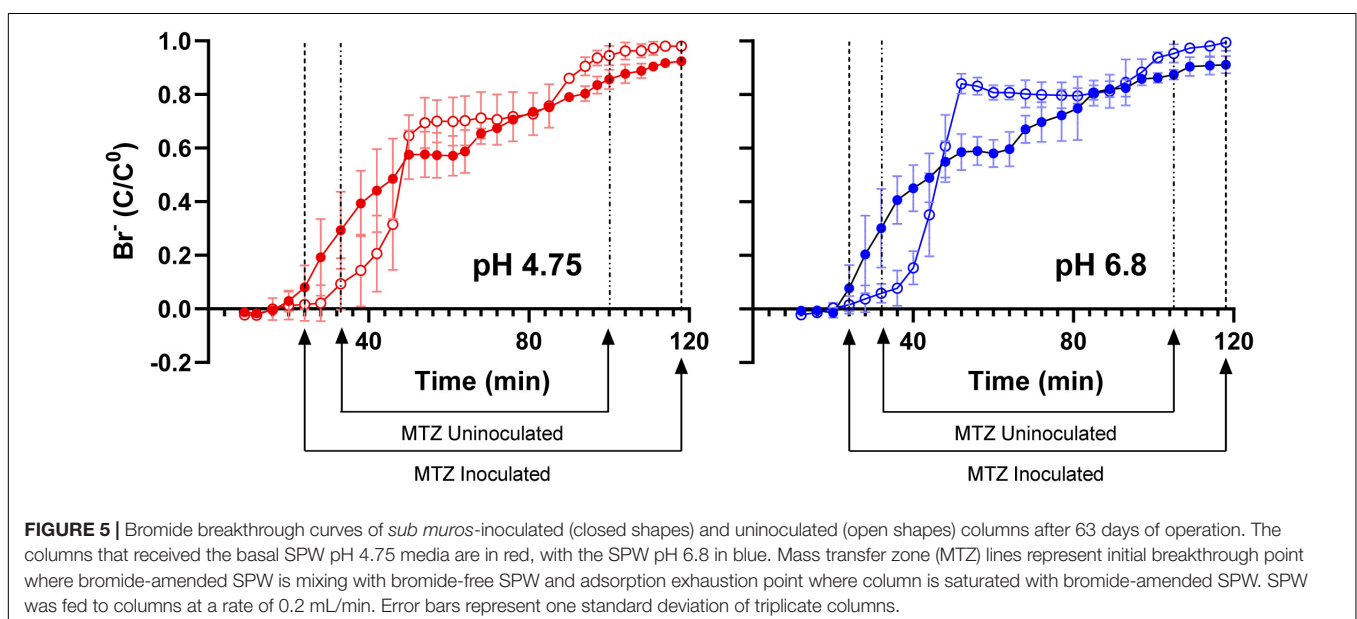
The microbial community composition in the batch incubations suggested that non-respiratory Fe(III) reduction could play a role in the observed iron reduction (Figure 3). To determine the extent of growth during column operation, we counted cells associated with the *sub muros* inoculum and at the conclusion of the column experiments. All the columns seeded with *sub muros* were initially inoculated at $\sim 9.2 \times 10^7$ cells/g. At 63 days, the population had increased in the columns at pH 4.75 by 4.3 \times , with the cell number in the pH 6.8 column increasing 4.6 \times . These data suggested an increase in microbial growth, and indeed the higher cell number in the pH 6.8 columns matches a higher-level of Fe(III) reduction. No microbial cells were detected in the uninoculated controls (Table 1).

DNA extraction from the inoculated columns produced sufficient DNA for Illumina sequencing, but repeated attempts to extract DNA from the uninoculated columns failed, matching the observations by direct cell counting. Illumina sequencing of the microbial communities in the columns matched our observations in batch culture (Figures 2, 3); there had been a shift from dominance by the Proteobacteria, to dominance by members of the Firmicutes. At the genus level, the columns were similarly dominated by members of *Clostridium*, *Desulfosporosinus*, and

Veillonella, which represented $\geq 90\%$ of the identified partial 16S rRNA gene sequences (Figure 3); however, members of the *Paenibacilli* were not observed. There was some inter-column variability under each of the pH conditions, particularly in regard to the dominance of *Clostridium* relative to *Desulfosporosinus* (Figure 3). In the *Desulfosporosinus*-dominated columns, we saw a darkening of the column material, which could indicate sulfidogenesis, but there was no decrease in the effluent sulfate concentration over the course of the incubations (Figures 4C,D). This suggests that while members of the *Desulfosporosinus* are accumulating in these columns, they may be functioning as Fe(III) reducers. Indeed, members of this genus have been shown to be the primary Fe(III) reducers under oligotrophic conditions (Nixon et al., 2017; Bomberg et al., 2019). Fe(III) reduction is widespread among the Clostridia, including a strain of *Clostridium beijerinckii* (Dobbin et al., 1999; Lehours et al., 2010; Shah et al., 2014; List et al., 2019). Indeed, in our previous batch cultures were capable of extensive (in some cases, complete) Fe(III) reduction (Parker et al., 2018), and Lentini et al. (2012) have demonstrated that *Clostridium*-enriched cultures are capable of extensive reduction of goethite- and hematite-Fe(III).

Microbially Induced Hydrologic Alterations of Canga Columns

Based on dissolved Fe(II) in column effluents, approximately 40 mg of $\text{Fe}(\text{OH})_3$ were removed from the columns due to microbiological Fe(III) reduction (Table 1). To determine if this export of mass impacted the hydraulic properties of the columns, we pumped bromide-amended SPW through the columns. Bromide breakthrough in the *sub muros*-inoculated columns preceded that of the uninoculated columns, and breakthrough was spread out in comparison to that of the uninoculated columns, which had a sharper curve (Figure 5). These observations indicate that flow through the uninoculated



columns did not experience the same mass transfer resistance seen in the columns in which microbiological Fe(III) reduction occurred (Lassabatere et al., 2004; Koestel et al., 2011; Safadoust et al., 2016). The porosity that allowed earlier bromide breakthrough is due to reductive dissolution of Fe(III) phases and export of dissolved Fe(II). In similar column experiments, Liang et al. (2019) found that bioreduction of sediment-associated Fe(III) led to the structural breakdown of particles in the columns and led to the earlier breakthrough of poorly-diffusible 2,6-difluorobenzoate. No change in more diffusible bromide breakthrough was observed after Fe(III) bioreduction (Liang et al., 2019). In the work presented here, Fe(III) bioreduction was more extensive, with maximal effluent Fe(II) concentrations of approximately 3 mM, in comparison to the maximal Fe(II) concentration of 0.3 mM observed by Liang et al. (2019). Taken together, the extensive Fe(III) bioreduction observed in these column experiments induced changes to the water flow paths in the packed canga.

Biogeochemical Implications

The results of our experiments indicate that the Fe(III) reducing activities of microorganisms associated with IFCs can induce reductive dissolution of Fe(III) phases, resulting in the transport of dissolved Fe(II) and hydrologic changes that are consistent with cave formation. While the Fe(III)-rich rocks of this region were generally considered to be resistant to weathering (Schuster et al., 2012; Monteiro et al., 2014), it is becoming increasingly clear that microbiological activities may induce extensive transformations to these rocks, especially canga (Parker et al., 2013, 2018; Levett et al., 2016, 2020; Gagen et al., 2018, 2019; Paz et al., 2020). Previous work has focused on the transformations of canga-Fe as a mechanism of canga permanence, whereby the weathering resistance of canga is owed to the alternating reductive dissolution of Fe(III) (hydr)oxides and abiotic or microbiological reoxidation of Fe(II) back to Fe(III) (Levett et al., 2016, 2020; Gagen et al., 2018, 2019, 2020; Paz et al., 2020). In this way, canga appears to be continuously weathering and reforming. The work here indicates that the Fe(III) rich phases could be more extensively weathered and removed from the systems, driven by the increased rates of Fe-reduction induced by water flow. Thus, Fe may be extensively mobilized from

rocks in the SE and QF by microbiological weathering via microbial Fe(III) reduction (either through respiratory activity or as an electron sink) and separation, which can be enhanced by groundwater flow. These results should be applicable to other iron formation areas in Brazil and help explain why caves are larger in the iron deposits of Carajás, in the wetter Amazon Basin (Auler et al., 2019). A positive feedback mechanism, in which fast infiltration water would lead to increased porosity and thus even faster water percolation could operate, enhancing the mass transfer mechanisms required to mobilize Fe(II). Our observations indicate that microorganisms associated with these systems are capable of robust Fe(III) reducing activity, which could induce sufficient reductive dissolution of Fe(III) phases to form a cave. The numerous caves of the SE and QF (> 3,000; Auler et al., 2019) indicate that the activity is extensive and continuously occurring. Indeed, we have observed remarkably high dissolved Fe concentrations in water circulating around caves in the QF (Parker et al., 2018). This extensive weathering of SE and QF Fe(III) phases may represent a previously underappreciated component of regional, and perhaps global Fe budgets.

DATA AVAILABILITY STATEMENT

The datasets presented in this study can be found in online repositories. The names of the repository/repositories and accession number(s) can be found in the article/supplementary material.

AUTHOR CONTRIBUTIONS

KC, MM, and TR carried out the lab work. JS, AA, CP, and HB carried out the fieldwork. All authors were involved in the design of the experiments and contributed to the manuscript.

FUNDING

This research was funded by the NSF grant #1645180 from NSF Geobiology and Low-temperature Geochemistry program to HB and JS.

REFERENCES

- Auler, A. S., Parker, C. W., Barton, H. A., and Soares, G. A. (2019). "Iron formation caves: genesis and ecology," in *Encyclopedia of Caves*, eds W. B. White, D. C. Culver, and T. Pipan (London: Academic Press), 559–566.
- Auler, A. S., Piló, L. B., Parker, C. W., Senko, J. M., Sasowsky, I. D., and Barton, H. A. (2014). "Hypogene cave patterns in iron ore caves: convergence of forms or processes," in *Hypogene Cave Morphologies*, eds K. Klimchou, I. D. Sasowsky, J. Mylroie, and A. S. Engel (Lewisburg, PA: Karst Waters Institute), 15–19.
- Benner, S. G., Hansel, C. M., Wielinga, B. W., Barber, T. M., and Fendorf, S. (2002). Reductive dissolution and biomineralization of iron hydroxide under dynamic flow conditions. *Environ. Sci. Technol.* 36, 1705–1711. doi: 10.1021/es0156441
- Beukes, N. J., Gutzmer, J., and Mukhopadhyay, J. (2003). The geology and genesis of high-grade hematite iron ore deposits. *Appl. Earth Sci.* 112, 18–25. doi: 10.1179/037174503225011243
- Bolyen, E., Rideout, J. R., Dillon, M. R., Bokulich, N. A., Abnet, C. C., Al-Ghalith, G. A., et al. (2019). Reproducible, interactive, scalable and extensible microbiome data science using QIIME 2. *Nat. Biotech.* 37, 852–857. doi: 10.1038/s41587-019-0209-9
- Bomberg, M., Claesson, L. L., Lamminmäki, T., and Kontula, A. (2019). Highly diverse aquatic microbial communities separated by permafrost in Greenland show distinct features according to environmental niches. *Front. Microbiol.* 10:1583. doi: 10.3389/fmicb.2019.01583
- Costa, T., and Sá, G. (2018). "Soft iron ores: geotechnical characteristics," in *Guidelines for Open Pit Slope Design in Weak Rocks*, eds D. Martin, and P. Stacey (Clayton South, VIC: CSIRO Publishing), 273–285.
- Cotta, M., and Forster, R. (2006). "The family *Lachnospiraceae*, including the genera *Butyrivibrio*, *Lachnospira* and *Roseburia*," in *The Prokaryotes*, Vol. 4, eds M. Dworkin, S. Falkow, E. Rosenberg, K. H. Schleifer, and E. Stackebrandt (New York, NY: Springer), 1002–1021.

- Dobbin, P. S., Carter, J. P., San Juan, C. G.-S., von Hobe, M., Powell, A. K., and Richardson, D. J. (1999). Dissimilatory Fe(III) reduction by *Clostridium beijerinckii* isolated from freshwater sediment using Fe(III) maltol enrichment. *FEMS Microbiol. Lett.* 176, 131–138. doi: 10.1111/j.1574-6968.1999.tb13653.x
- Dorr, J. V. N. (1964). Supergene iron ores of Minas Gerais, Brazil. *Econ. Geol.* 59, 1203–1240. doi: 10.2113/gsecongeo.59.7.1203
- Downs, R. T., and Hall-Wallace, M. (2003). The American Mineralogist crystal structure database. *Am. Mineral.* 88, 247–250.
- Gagen, E. J., Levett, A., Paz, A., Bostlemann, H., da Silva Valadares, R. B., Bitencourt, J. A. P., et al. (2020). Accelerating microbial iron cycling promotes re-cementation of surface crusts in iron ore regions. *Microb. Biotechnol.* 13, 1960–1971. doi: 10.1111/1751-7915.13646
- Gagen, E. J., Levett, A., Paz, A., Gustauer, M., Caldeira, C. F., da Silva Valadares, R. B., et al. (2019). Biogeochemical processes in canga ecosystems: armoring of iron ore against erosion and importance in iron duricrust restoration in Brazil. *Ore Geol. Rev.* 107, 573–586. doi: 10.1016/j.oregeorev.2019.03.013
- Gagen, E. J., Levett, A., Shuster, J., Fortin, D., Vasconcelos, P. M., and Southam, G. (2018). Microbial diversity in actively forming iron oxides from weathered banded iron formation systems. *Microbes Environ.* 33, 385–393. doi: 10.1264/j sme2.ME18019
- Gonzalez-Gil, G., Amonette, J. E., Romine, M. F., Gorby, Y. A., and Geesey, G. G. (2005). Bioreduction of natural specular hematite under flow conditions. *Geochem. Cosmochim. Acta* 69, 1145–1155. doi: 10.1016/j.gca.2004.08.014
- Hansel, C. M., Benner, S. G., and Fendorf, S. (2005). Competing Fe(II)-induced mineralization pathways of ferrihydrite. *Environ. Sci. Technol.* 29, 7147–7153. doi: 10.1021/es050666z
- Hansel, C. M., Benner, S. G., Neiss, J., Dohnalkova, A., Kukkadapu, R. K., and Fendorf, S. (2003). Secondary mineralization pathways induced by dissimilatory iron reduction of ferrihydrite under advective flow. *Geochem. Cosmochim. Acta* 67, 2977–2992. doi: 10.1016/S0016-7037(03)00276-X
- Hansel, C. M., Lentini, C. J., Tang, Y., Johnston, D. T., Wankel, S. D., and Jardine, P. M. (2015). Dominance of sulfur-fueled iron oxide reduction in low-sulfate freshwater sediments. *ISME J.* 9, 2400–2412. doi: 10.1038/ismej.2015.50
- Hershey, O. S., Kallmeyer, J., Wallace, A., Barton, M. D., and Barton, H. A. (2018). High microbial diversity despite extremely low biomass in a deep karst aquifer. *Front. Microbiol.* 9:2823. doi: 10.3389/fmicb.2018.02823
- Igarashi, K., and Kato, S. (2021). Reductive transformation of Fe(III) (oxyhydr)oxides by mesophilic momoacetogens in the genus *Sporomusa*. *Front. Microbiol.* 12:600808. doi: 10.3389/fmicb.2021.600808
- Johnson, D. B., Kanao, T., and Hedrich, S. (2012). Redox transformations of iron at extremely low pH: fundamental and applied aspects. *Front. Microbiol.* 3:96. doi: 10.3389/fmicb.2012.00096
- Kato, S., Yumoto, I., and Kamagata, Y. (2015). Isolation of acetogenic bacteria that induce biocorrosion by utilizing metallic iron as the sole electron donor. *Appl. Environ. Microbiol.* 81, 67–73. doi: 10.1128/AEM.02767-14
- Koestel, J. K., Moeys, J., and Jarvis, N. J. (2011). Meta-analysis of the effects of soil properties, site factors and experimental conditions on preferential solute transport. *Hydrol. Earth Syst. Sci. Discuss.* 8, 10007–10052. doi: 10.5194/hessd-8-10007-2011
- Lassabatere, L., Winiarski, T., and Galvez-Cloutier, R. (2004). Retention of three heavy metals (Zn, Pb, and Cd) in a calcareous soil controlled by the modification of flow with geotextiles. *Environ. Sci. Technol.* 38, 4215–4221. doi: 10.1021/es035029s
- Lehours, A.-C., Rabiet, M., Morel-Desrosiers, N., Morel, J.-P., Jouve, L., Arbeille, B., et al. (2010). Ferric iron reduction by fermentative strain BS2 isolated from an iron-rich anoxic environment (Lake Pavin, France). *Geomicrobiol. J.* 27, 714–722. doi: 10.1080/01490451003597663
- Lentini, C. J., Wankel, S. D., and Hansel, C. M. (2012). Enriched iron(III)-reducing bacterial communities are shaped by carbon substrate and iron oxide mineralogy. *Front. Microbiol.* 3:404. doi: 10.3389/fmicb.2012.00404
- Levett, A., Gagen, E., Shuster, J., Rintoul, L., Tobin, M., Vongsvivut, J., et al. (2016). Evidence of biogeochemical processes in iron duricrust formation. *J. S. Am. Earth Sci.* 71, 131–142. doi: 10.1016/j.jsames.2016.06.016
- Levett, A., Vasconcelos, P. M., Gagen, E. J., Rintoul, L., Spier, C., Guagliardo, P., et al. (2020). Microbial weathering signatures in lateritic ferruginous duricrusts. *Earth Planet. Sci. Lett.* 538:116209. doi: 10.1016/j.epsl.2020.116209
- Liang, X., Radosevich, M., Löffler, F., Schaeffer, S. M., and Zhuang, J. (2019). Impact of microbial iron oxide reduction on the transport of diffusible tracers and non-diffusible nanoparticles in soils. *Chemosphere* 220, 391–402. doi: 10.1016/j.chemosphere.2018.12.165
- List, C., Hosseini, Z., Meibom, K. L., Hatzimanikatis, V., and Bernier-Latmani, R. (2019). Impact of iron reduction on the metabolism of *Clostridium acetobutylicum*. *Environ. Microbiol.* 21, 3548–3563. doi: 10.1111/1462-2920.14640
- Lovley, D. R., and Phillips, E. J. P. (1987). Rapid assay for microbially reducible ferric iron in aquatic sediments. *Appl. Environ. Microbiol.* 53, 1536–1540. doi: 10.1128/aem.53.7.1536-1540.1987
- Loyaux-Lawniczak, S., Vuilleumier, S., and Geoffroy, V. A. (2019). Efficient reduction of iron oxides by *Paenibacillus* spp. strains isolated from tropical soils. *Geomicrobiol. J.* 36, 423–432. doi: 10.1080/01490451.2019.1566415
- Mesquita, D. C., Dantas, J. C. M., Paula, R. S., and Guerra, K. J. (2017). Estudo dos parâmetros hidrocinâmicos obtidos em ensaios de campo em itabiritos bandos da porção sudoeste do Quadrilátero Ferrífero, MG. *Geonomos* 25, 12–19.
- Minyard, M. L., and Burgos, W. D. (2007). Hydrologic flow controls on biologic iron(III) reduction in natural sediments. *Environ. Sci. Technol.* 41, 1218–1224. doi: 10.1021/es0619657
- Monteiro, H. S., Vasconcelos, P. M., Farley, K. A., Spier, C. A., and Mello, C. L. (2014). (U-Th)/He geochronology of goethite and the origin and evolution of cangas. *Geochim. Cosmochim. Acta* 131, 267–289. doi: 10.1016/j.gca.2014.01.036
- Nixon, S. L., Telling, J. P., Wadham, J. L., and Cockell, C. S. (2017). Viable cold-tolerant iron-reducing microorganisms in geographically diverse subglacial environments. *Biogeosciences* 14, 1445–1455. doi: 10.5194/bg-14-1445-2017
- Parker, C. W., Auler, A. S., Barton, M. D., Sasowsky, I. D., Senko, J. M., and Barton, H. A. (2018). Fe (III) reducing microorganisms from iron ore caves demonstrate fermentative Fe (III) reduction and promote cave formation. *Geomicrobiol. J.* 35, 311–322. doi: 10.1080/01490451.2017.1368741
- Parker, C. W., Wolf, J. A., Auler, A. S., Barton, H. A., and Senko, J. M. (2013). Microbial reducibility of Fe (III) phases associated with the genesis of iron ore caves in the Iron Quadrangle, Minas Gerais, Brazil. *Minerals* 3, 395–411. doi: 10.3390/min3040395
- Paz, A., Gagen, E. J., Levett, A., Zhao, Y., Kopitke, P. M., and Southam, G. (2020). Biogeochemical cycling of iron oxides in the rhizosphere of plants grown on ferruginous duricrust (canga). *Sci. Total Environ.* 713:136637. doi: 10.1016/j.scitotenv.2020.136637
- Rainey, F. A. (2009). “Family V. *Lachnospiraceae* fam. nov,” in *Bergey’s Manual of Systematic Bacteriology*, Vol. 3, eds P. De Vos, G. M. Garrity, D. Jones, N. R. Krieg, W. Ludwig, F. A. Rainey, et al. (Dordrecht: Springer), 921–968.
- Roden, E. E. (2004). Analysis of long-term bacterial vs. chemical Fe(III) oxide reduction kinetics. *Geochem. Cosmochim. Acta* 68, 3205–3216. doi: 10.1016/j.gca.2004.03.028
- Roden, E. E. (2006). Geochemical and microbiological controls on dissimilatory iron reduction. *C. R. Geosci.* 338, 456–467. doi: 10.1016/j.crte.2006.04.009
- Roden, E. E., and Urrutia, M. M. (1999). Ferrous iron removal promotes microbial reduction of crystalline iron(III) oxides. *Environ. Sci. Technol.* 33, 1847–1853. doi: 10.1021/es9809859
- Roden, E. E., and Urrutia, M. M. (2002). Influence of biogenic Fe(II) on bacterial crystalline Fe(III) oxide reduction. *Geomicrobiol. J.* 19, 209–251. doi: 10.1080/01490450252864280
- Roden, E. E., Urrutia, M. M., and Mann, C. J. (2000). Bacterial reductive dissolution of crystalline Fe(III) oxide in continuous-flow column reactors. *Appl. Environ. Microbiol.* 66, 1062–1065. doi: 10.1128/AEM.66.3.1062-1065.2000
- Roden, E. E., and Zachara, J. M. (1996). Microbial reduction of crystalline iron(III) oxides: influence of oxide surface area and potential for cell growth. *Environ. Sci. Technol.* 30, 1618–1628. doi: 10.1021/es9506216
- Rolim, V. K., Rosière, C. A., Santos, J. O. S., and McNaughton, N. J. (2016). The Orosirian-Statherian banded iron formation-bearing sequences of the southern border of the Espinhaço Range, Southeast Brazil. *J. S. Am. Earth Sci.* 65, 43–66. doi: 10.1016/j.jsames.2015.11.003
- Rosière, C., Bekker, A., Rolim, V., and Santos, J. (2019). Post-Great Oxidation Event Orosirian–Statherian iron formations on the São Francisco craton: geotectonic implications. *I. Arc* 28:e12300. doi: 10.1111/iar.12300
- Royer, R. A., Dempsey, B. A., Jeon, B.-H., and Burgos, W. D. (2004). Inhibition of biological reductive dissolution of hematite by ferrous iron. *Environ. Sci. Technol.* 38, 187–193. doi: 10.1021/es026466u

- Safadoust, A., Khaboushan, E. A., Mahboubi, A. A., Gharabaghi, B., Mosaddeghi, M. H., Ahrens, B., et al. (2016). Comparison of three models describing bromide transport affected by different soil structure types. *Arch. Agron. Soil Sci.* 62, 674–687. doi: 10.1080/03650340.2015.1074184
- Sass, H., Overmann, J., Rütters, H., Babenzien, H.-D., and Cypionka, H. (2004). *Desulfosporomusa polytropa* gen. nov., sp. nov., a novel sulfate-reducing bacterium from sediments of an oligotrophic lake. *Arch. Microbiol.* 182, 204–211. doi: 10.1007/s00203-004-0703-3
- Sato, Y., Hamai, T., Hori, T., Aoyagi, T., Inaba, T., Kobayashi, M., et al. (2019). *Desulfosporosinus* spp. were the most predominant sulfate-reducing bacteria in pilot- and laboratory-scale passive bioreactors for acid mine drainage treatment. *Appl. Microbiol. Biotechnol.* 103, 7783–7793. doi: 10.1007/s00253-019-10063-2
- Schuster, D. L., Farley, K. A., Vasconcelos, P. M., Balco, G., Monteiro, H. S., Waltenberg, K., et al. (2012). Cosmogenic ^3He in hematite and goetite from Brazilian canga duricrust demonstrates the extreme stability of these surfaces. *Earth Planet. Sci. Lett.* 329–330, 41–50. doi: 10.1016/j.epsl.2012.02.017
- Senko, J. M., Zhang, G., McDonough, J. T., Bruns, M. A., and Burgos, W. D. (2009). Metal reduction at low pH by a *Desulfosporosinus* species: implications for the biological treatment of acidic mine drainage. *Geomicrobiol. J.* 26, 71–82. doi: 10.1080/01490450802660193
- Shah, M., Lin, C.-C., Kukkadapu, R., Engelhard, M. H., Zhao, X., Wang, Y., et al. (2014). Syntrophic effects in a subsurface Clostridial consortium on Fe(III)-(oxyhydr)oxide reduction and secondary mineralization. *Geomicrobiol. J.* 31, 101–115. doi: 10.1080/01490451.213.806601
- Silveira Braga, F. C., Rosière, C. A., Schneider Santos, J. O., Hagemann, S. G., Danyushevsky, L., and Valle Salles, P. (2021). Geochemical and tectonic constraints on the genesis of iron formation-hosted magnetite-hematite deposits at the Guanhões Block (Brazil) by contact metasomatism with pegmatite intrusions. *Ore Geol. Rev.* 129:103931. doi: 10.1016/j.oregeorev.2020.103931
- Smith, A. J. B. (2015). The life and times of banded iron formations. *Geology* 43, 1111–1112. doi: 10.1130/focus122015.1
- Souza, A., Figueiredo e Silva, R., Rosière, C., Dias, G., and Morais, F. (2015). Estudos geoquímicos de iabiritos da Serra do Sapo, espinhaço meridional, Minas Gerais. *Rev. Geonomos* 22, 1–17. doi: 10.18285/geonomos.v22i2.313
- Spier, C. A., de Oliveira, S. M. B., Sial, A. N., and Rios, F. J. (2007). Geochemistry and genesis of the banded iron formations of the Cauê Formation, Quadrilátero Ferrífero, Minas Gerais, Brazil. *Precambrian Res.* 152, 170–206. doi: 10.1016/j.precambres.2006.10.003
- Spier, C. A., Levett, A., and Rosière, C. A. (2018). Geochemistry of canga (ferricrete) and evolution of the weathering profile developed on itabirite and iron ore in the Quadrilátero Ferrífero, Minas Gerais, Brazil. *Miner. Depos.* 54, 983–1010. doi: 10.1007/s00126-018-0856-7
- Stookey, L. L. (1970). Ferrozine—a new spectrophotometric reagent for iron. *Anal. Chem.* 42, 779–781.
- Urrutia, M. M., Roden, E. E., and Zachara, J. M. (1999). Influence of aqueous and solid-phase Fe(II) complexants on microbial reduction of crystalline iron(III) oxides. *Environ. Sci. Technol.* 33, 4022–4028. doi: 10.1021/es990447b
- Weber, K. A., Achenbach, L. A., and Coates, J. D. (2006). Microorganisms pumping iron: anaerobic microbial iron oxidation and reduction. *Nat. Rev. Microbiol.* 4, 752–764. doi: 10.1038/nrmicro1490
- Wefer-Roehl, A., and Kübeck, C. (2014). *Guidelining Protocol for Soil-Column Experiments Assessing Fate and Transport of Trace Organics.* 308339. Available online at: [http://demeau-fp7.eu/sites/files/D123a Guidelines Column experiments.pdf](http://demeau-fp7.eu/sites/files/D123a%20Guidelines%20Column%20experiments.pdf) (accessed June 14, 2018).

Conflict of Interest: The authors declare that the research was conducted in the absence of any commercial or financial relationships that could be construed as a potential conflict of interest.

Copyright © 2021 Calapa, Mulford, Rieman, Senko, Auler, Parker and Barton. This is an open-access article distributed under the terms of the Creative Commons Attribution License (CC BY). The use, distribution or reproduction in other forums is permitted, provided the original author(s) and the copyright owner(s) are credited and that the original publication in this journal is cited, in accordance with accepted academic practice. No use, distribution or reproduction is permitted which does not comply with these terms.